Research in Astronomy and Astrophysics, 22:105007 (9pp), 2022 October https://doi.org/10.1088/1674-4527/ac833a


# A Search Technique Based on Deep Learning for Fast Radio Bursts and Initial Results for FRB 20201124A with the NSRT

Yan-Ling Liu[1,2,3,4], Jian Li[1,3,4], Zhi-Yong Liu[1,3], Mao-Zheng Chen[1,3,4], Jian-Ping Yuan[1,3], Na Wang[1,3], Rai Yuen[1], and Hao Yan[1,3,4]

[1] Xinjiang Astronomical observatory, Chinese Academy of Sciences, Urumqi 830011, China; chen@xao.ac.cn, liuyanling@xao.ac.cn
[2] University of Chinese Academy of Sciences, Beijing 100049, China
[3] Key Laboratory of Radio Astronomy, Chinese Academy of Sciences, Nanjing 210033, China
[4] Xinjiang Key Laboratory of Microwave Technology, Urumqi 830011, China
*Received 2022 May 12; revised 2022 June 24; accepted 2022 July 11; published 2022 September 28*

## Abstract

The origin and phenomenology of Fast Radio Bursts (FRBs) remain unknown. Fast and efficient search technology for FRBs is critical for triggering immediate multi-wavelength follow-up and voltage data dump. This paper proposes a dispersed dynamic spectra search (DDSS) pipeline for FRB searching based on deep learning, which performs the search directly from observational raw data, rather than relying on generated FRB candidates from single-pulse search algorithms that are based on de-dispersion. We train our deep learning network model using simulated FRBs as positive and negative samples extracted from the observational data of the Nanshan 26 m radio telescope (NSRT) at Xinjiang Astronomical Observatory. The observational data of PSR J1935+1616 are fed into the pipeline to verify the validity and performance of the pipeline. Results of the experiment show that our pipeline can efficiently search single-pulse events with a precision above 99.6%, which satisfies the desired precision for selective voltage data dump. In March 2022, we successfully detected the FRBs emanating from the repeating case of FRB 20201124A with the DDSS pipeline in *L*-band observations using the NSRT. The DDSS pipeline shows excellent sensitivity in identifying weak single pulses, and its high precision greatly reduces the need for manual review.

*Key words:* radio continuum: general – methods: data analysis – methods: observational

## 1. Introduction

Fast radio bursts (FRBs) are bright, highly dispersed, millisecond-duration cosmological radio transients (see Cordes & Chatterjee 2019; Petroff et al. 2019; Zhang 2020 for reviews). The transient radio phenomenon was first discovered by Lorimer et al. (2007) during a search in the archival data of the Parkes multibeam pulsar survey at the Parkes observatory. Thornton et al. (2013) reported the findings of four more high-dispersion measure (DM) bursts in other surveys with the Parkes 64 m radio telescope, which showed similar observed characteristics to the Lorimer burst. At that point, FRBs became widely accepted as a newly recognized astrophysical phenomenon (Amiri et al. 2018). However, because of their short-duration and rare repetition, it is very difficult to capture them. Nowadays, FRBs represent one of the new and most exciting mysteries in astrophysics. So far, except for FRB 200428, which was the first to be confirmed as originating from the Galactic magnetar soft gamma repeater (SGR) SGR J1935 +2154 (Li et al. 2021), the origins of FRBs are still unknown and at present the source class is defined only through observations (Petroff et al. 2019).

With rapidly growing enthusiasm for FRB research in recent years, many new FRB events have been discovered in observations not only with the Parkes telescope, but also from other telescopes all over the world. The latter include the Arecibo telescope (Spitler et al. 2014), the Green Bank Telescope (GBT) (Masui et al. 2015), the Upgraded Molonglo Synthesis Telescope (UTMOST) (Caleb et al. 2016; Farah et al. 2019), the Australian Square Kilometer Array Pathfinder (ASKAP) (Bannister et al. 2017; Shannon et al. 2018), the Canadian Hydrogen Intensity Mapping Experiment (CHIME) (Amiri et al. 2019, 2021), the Effelsberg telescope (Marcote et al. 2020), the Sardinia Radio Telescope (SRT) (Pilia et al. 2020) and the Five-hundred-meter Aperture Spherical radio Telescope (FAST) (Zhu et al. 2020; Niu et al. 2021). The detection rate of FRBs is rapidly increasing, and even thousands were detected in one year. From 2018 July 25 to 2019 July, 536 FRBs were detected by CHIME (Amiri et al. 2021). At FAST, 1652 independent bursts from FRB 121102 were detected in 59.5 hr spanning over 47 days (Li et al. 2021), and 1863 polarized bursts from the repeating source FRB 202011124A were detected in 88 hr over 54 days (Xu et al. 2022). FRBs are already being used to probe the halos of other galaxies and to address the distribution of baryons in the intergalactic medium (IGM) (Chatterjee 2021), raising the need for more FRBs for further research. Many more telescopes in

the coming years will join the FRB search or multi-wavelength coordinated observations. The observational data of FRB searches will continue to increase at an explosive rate. The issues we are facing with the speed and storage for large data processing will be more difficult.

Searching for FRBs from observational data is usually done with de-dispersion based single-pulse algorithms such as HEIMDALL (Barsdell et al. 2012), PRESTO (Ransom 2001), FDMT (Bannister et al. 2017), CDMT (Bassa et al. 2017) and BEAR (Men et al. 2019). These algorithms have also been embedded in real-time FRB search systems or backends for online searching. Examples include the CHIME/FRB real-time search system with bonsai (Amiri et al. 2018), GREENBURST with HEIMDALL on GBT (Agarwal et al. 2020b) and the piggyback with BEAR (Men et al. 2019). These algorithms are easily triggered by noise and radio frequency interference (RFI). The false positive rate in the candidates is too high to be manually inspected. Currently, machine learning is being used to provide an automated solution to reduce the sheer volume of false positives. Wagstaff et al. (2016), Farah et al. (2019), Foster et al. (2018) and Michilli et al. (2018) applied traditional machine learning to the classification of single-pulse transient candidate classification. Connor & van Leeuwen (2018), Zhang et al. (2018) and Agarwal et al. (2020a) utilized the deep learning model for FRB searches. In addition, the application of artificial intelligence (AI) to automate the classification of FRB candidates can realize real-time FRB search and provide high-precision and high-speed prerequisites for near-real-time voltage dumps, which are very valuable for FRB research. Voltage capture not only leads to superior localization for an FRB, but it also gives remarkable temporal and frequency resolution for off-line analysis (Farah et al. 2019).

Compared with traditional machine learning methods, deep learning does not require spending lots of time on feature engineering. This avoids the subjectivity and incompleteness caused by artificial design and selection of features. In addition, the learning ability of deep learning for large data sets has far exceeded that of traditional machine learning. Past research has shown that, for the classification of FRB candidates, a deep learning model could achieve better outcomes. In this paper, we develop a direct dispersed dynamic spectra search (DDSS) pipeline for observational raw data based on deep learning. The rest of this paper is organized in the following manner. In Section 2, we outline the process flow of the FRB search pipeline. In Section 3, we detail our data preparation for the deep learning models. In Section 4, we describe the method for acquiring the deep learning classifier. In Section 5, we test our pipeline and describe the bursts from the repeating case of FRB 20201124A detected with the Nanshan 26 m radio telescope (NSRT). Finally, in Section 6, we summarize our main conclusions and provide a brief outlook for the future work of the DDSS pipeline.

## 2. The DDSS Pipeline

In previous studies, FRB classifiers based on machine learning were mostly used to identify and classify FRB candidates produced by an automatic search pipeline that implements the dispersive algorithm. Connor & van Leeuwen (2018) suggested replacing the de-dispersion backend with a deep neural network (DNN) classifier for executing transient detection. The de-dispersion process of repeated trials with different DMs and converting the dynamic spectrum data into DM-time intensity are computationally expensive. The direct deep learning detection can save time and hardware resources, and also avoids the deviation risk caused by traditional de-dispersion algorithm in searching FRBs. Zhang et al. (2018) presented a direct FRB detection method based on a very deep convolutional neural network, named residual network. Using this network, they found 72 new pulses of FRB 121102 in a 5 hr observation at *C*-band, where 21 bursts were previously detected. They demonstrated its advantage over a traditional brute-force de-dispersion algorithm in terms of higher sensitivity, lower false positive rates and faster computational speed. Based on the above experience, we developed the DDSS pipeline for direct deep learning detection of FRBs from observational raw data produced by the NSRT. The simplified schematic drawing for the search pipeline system is illustrated in Figure 1.

We divide the observational raw spectrogram data into frames, each with a fixed number of samples along the time axis, then preprocess them and feed them into the deep learning classifier for prediction. Here, we set the classification threshold to 0.5. When the deep learning classifier outputs a probability above the fixed threshold value, the pipeline will write the data of the candidate to a separate file on a disk and store the time-frequency plot of the FRB event candidate for offline analysis and visual inspection. At the same time, the researchers will receive an email notification of the newly detected FRB event candidate.

## 3. Data Preparation

### *3.1. Data Set*

The deep learning classifier is directly used to search for FRB events in the observational spectrogram data. Essentially, it is an application for binary classification between FRBs and background noise that contains some RFI. Two classes of samples are needed to build a training set: the positive frames and the negative frames. The negative frames can be randomly extracted from the observational data. Because of the limited population of FRBs, it is not possible to provide a comprehensive data set for training a deep learning model. In view of the simple morphology of FRBs, however, it is straightforward to build a data set of FRBs by means of simulation. Simulated FRBs have been used in multiple

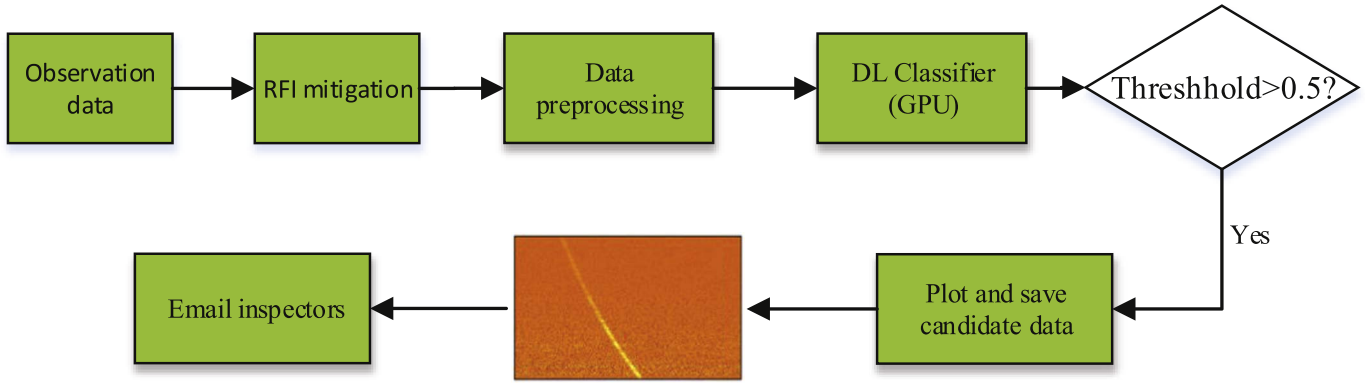


**Figure 1.** The schematic drawing of the DDSS FRB search pipeline system.

scenarios successfully. Farah et al. (2019) applied the simulated FRBs to evaluate the performance of the machine learning classifier. Amiri et al. (2021) developed an injection system with the internally-developed simpulse[5] library to quantify the biases in their instrumental and software detection pipeline. Connor & van Leeuwen (2018), Zhang et al. (2018) and Agarwal et al. (2020a) also utilized simulated FRBs to train their deep learning models.

Radio bursts traveling through the ionized interstellar medium and captured by ground-based telescopes will show some propagation effects, such as dispersive delay, scintillation, scattering and Faraday rotation. These effects are related to the morphological characteristics of the radio bursts in the two-dimensional spectrograms. Through simulation, we can control the required parameters for an ideal acquisition of a data set that captures all the variations in DM, scattering, smearing, amplitude, width, scintillation pattern and so on. We injected simulated FRB pulses into the negative frames to generate positive FRB samples. In this paper, we adopt the simulation algorithm designed by Zhang et al. (2018), but with certain details changed. For example, the scatter width is much wider in our *L*-band observation than that in their *C*-band observation.

The observational data used in this paper were produced by the *L*-band receiver and XFB backend of the NSRT at Xinjiang Astronomical Observatory (XAO). The data are two-dimensional spectrograms across the 512 MHz bandwidth with the frequency resolution of 1 MHz and a sampling time of 64 μs. Because the *L*-band receiver only covers a bandwidth of 320 MHz (1400–1720 MHz), the extra pixels of the spectrograms are trimmed out.

The simulated FRBs that are fed into the deep learning model are in the form of the dynamic spectrograms without dedispersion. Here, we set each frame with 2048 consecutive samples. Instead of using DM values that are too high, we built a simulated FRB set with DM merely ranging from 100 to 500 pc cm$^{-3}$ for our current application. We also set the arrival time for each burst with a random value chosen from a specified range to simulate the variable distribution of pulses in the frame. Figure 2 shows some examples of the simulated FRBs.

### 3.2. Data Pre-processing

The input data must be preprocessed before being fed into the deep learning network model. The preprocessing mainly includes RFI mitigation, size-trimming, normalization and down-sampling. RFI is rapidly becoming a major issue in radio astronomy, which is ubiquitous especially at *L*-band and below. RFI comes from various sources and shows diversity, which present a great challenge to astronomical observations. In our experiments, pronounced RFI characteristics can even be misinterpreted as the focus of learning for the network model making the real characteristics of FRBs be ignored. Therefore, it is necessary to perform RFI mitigation before inputting the data into the deep learning network. Although many methods have been developed to mitigate RFI, there is no general method to mitigate all kinds of RFI. RFI can be persistent or impulsive as well as broad-band or narrow-band. In this paper, channel-zapping is used to remove the persistent RFI that contaminates the 1450–1465 MHz and 1535–1545 MHz frequency bands. Second, IQRM (Morello et al. 2022) is integrated to derive a time-variable frequency channel mask for short-duration narrow-band RFI. In addition, an improved version of zero-DM filter (Eatough et al. 2009), called the zero-DM matched filter (ZDMF) proposed by Men et al. (2019), is applied to remove more short-duration broad-band RFI. The examples of RFI mitigation in our data are displayed in Figure 3.

All input data need to be uniform in size. We trimmed out the extra part of the input data beyond the bandwidth of the *L*-band receiver, normalized them to zero mean and unity

[5] https://github.com/kmsmith137/simpulse

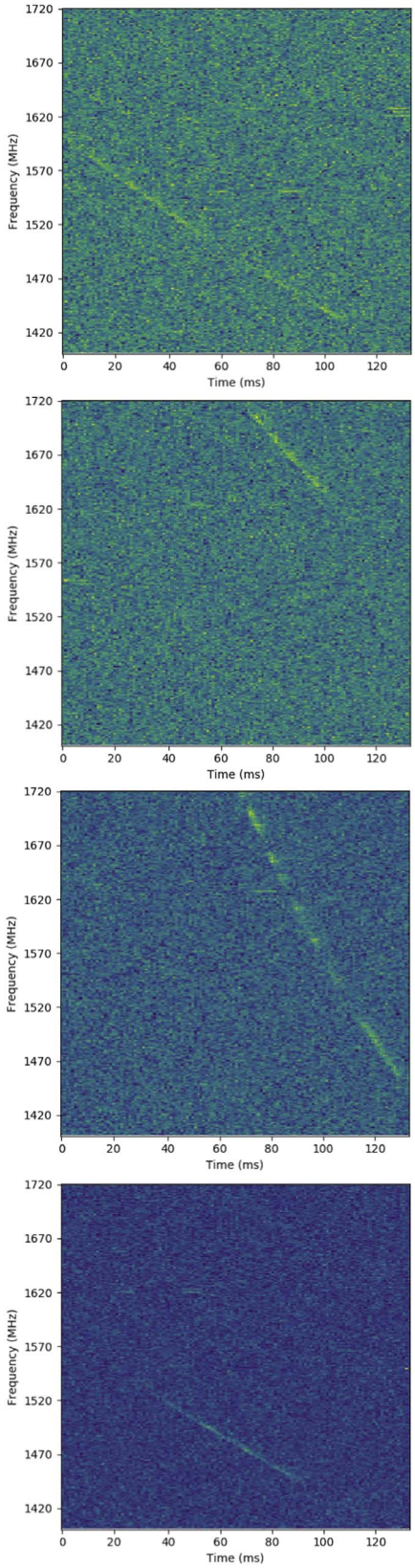


**Figure 2.** The examples of simulated FRBs on observations.

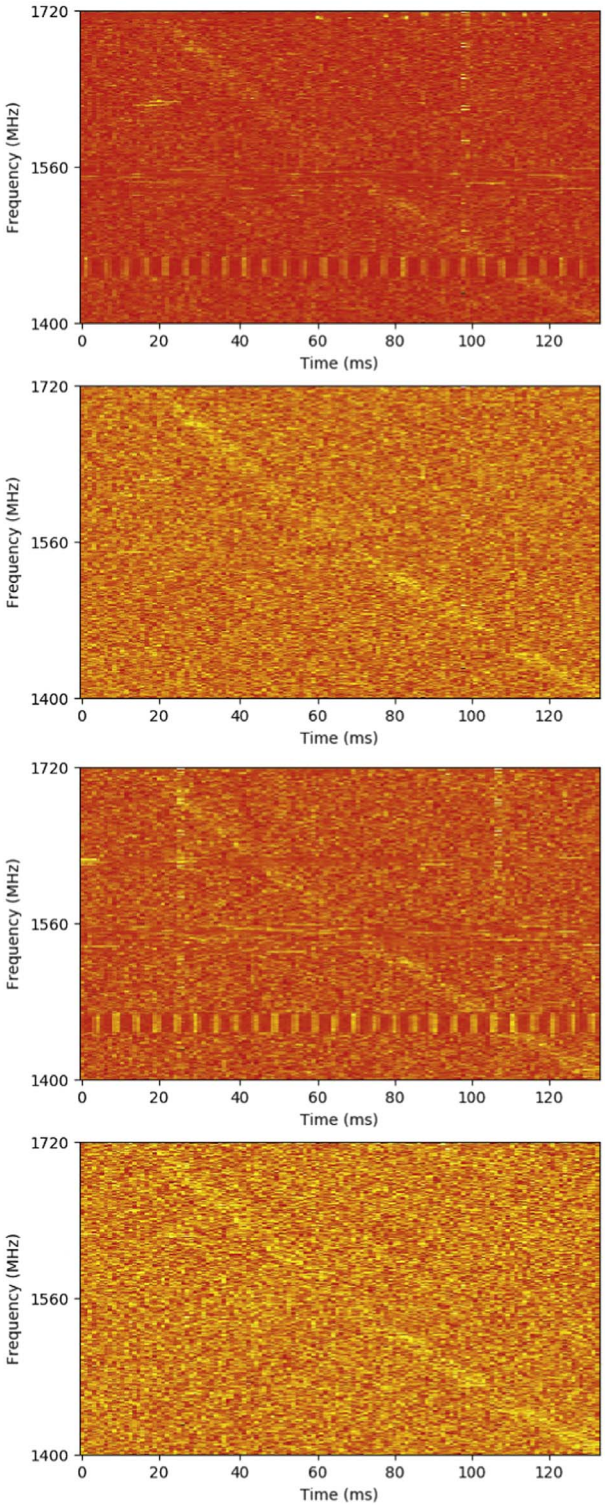


**Figure 3.** Two examples of RFI mitigation results. The top panel displays the observational data of PSR J1935+1616, which have been contaminated by persistent and short duration RFI. The bottom panel features the same data set after RFI mitigation, and the astronomical signals with the dispersion characteristic are well preserved.

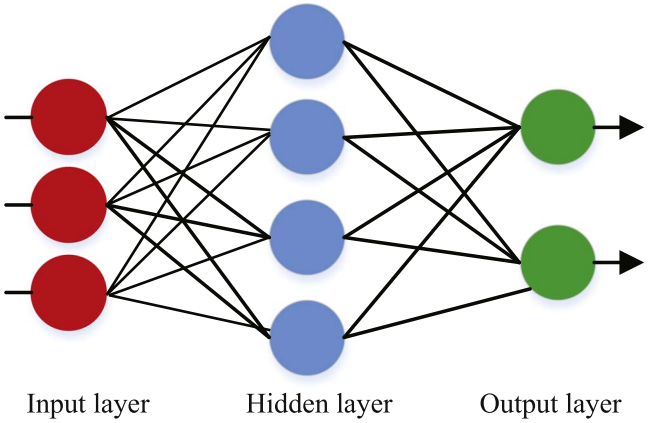


**Figure 4.** A schematic diagram for a simple neural network structure.

standard deviation, and then performed the down-sampling process on them to improve the signal-to-noise ratio (S/N). Finally, the preprocessed spectrogram data with a fixed size ($320 \times 128$) are fed into the network model.

## 4. Deep Learning-based Classifier

### *4.1. Network Models*

In recent years, deep learning has made breakthrough progress due to the development of the computing and GPU technology. The concept of deep learning originates from an artificial neural network, which is essentially a complex and deep hierarchical neural network algorithm model established from imitation of a human brain. Figure 4 depicts a simple neural network structure, which consists of an input layer, a hidden layer and an output layer. A deeper neural network model can be built with increasing number of hidden layers. However, such typical and fully connected DNNs with excessive parameters will encounter training difficulty. Therefore, in order to overcome the problem of gradient disappearance or explosion in the training, different types of deep learning models have been developed. Convolutional neural network, as one of the representative deep learning algorithms, has gained remarkable achievements in the field of image detection and recognition. Convolutional neural network is a kind of feed-forward neural network with deep structure and convolution computation. Its main feature is that the convolution layer and the pooling layer are added to the general neural network to form the feature extractor. Its basic structure includes the input layer, convolution layer, activation function layer, pooling layer, full connection layer and output layer, as illustrated in Figure 5. The convolution layer, activation function layer, pooling layer and full connection layer correspond to the hidden layer of the neural network. The input layer is used for data entry. The convolution layer and activation layer are used to realize feature extraction and feature nonlinear mapping of local areas in the previous layer, so as to realize local connection and weight sharing and reduce the number of parameters. Pooling layer is used to compress the size of data and parameters to reduce overfitting. The full connection layer is utilized for re-fitting to reduce the loss of characteristic information. Finally, the results are output through the output layer.

At present, many convolutional neural network models with different structures have been developed in response to different application requirements and continuous practice. In this paper, we use Keras (Chollet et al. 2015) with the TensorFlow (Abadi et al. 2016) back-end to quickly build our network models. Due to the simple morphological characteristics of FRBs, we choose the 18-layer ResNetv2 (ResNet18v2) and Xception (Chollet 2016), which are relatively simple network models with fewer layers to train. ResNet was first proposed by He et al. (2016a), which uses a residual block with shortcut connections to solve the problem related to the degradation in training precision as the model layers increase. He et al. (2016b) changed the residual block structure of ResNet from Conv-BN-ReLU to BN-ReLU-Conv to improve the performance. The improved ResNet was called ResNetv2. Xception signifies the extreme version of Inception (Chollet et al. 2015), which replaces the standard Inception modules with depthwise separable convolutions. Comparing with Inception, Xception presents better performance without increasing the complexity of a network model. Keras also provides some models with weights pre-trained on ImageNet, such as Xception, VGG16/19 (Simonyan & Zisserman 2014), ResNet50/101/152, DenseNet121/169/201 (Huang et al. 2017) and so on. We directly imported Xception, VGG16 and VGG19 with random weights to perform the training experiments, with each experiment having the same training set. The results show that the Xception model achieves the best training performance in our experiments.

### *4.2. Model Evaluation*

To reduce the voltage dump and manual workload for our application, we aimed to accurately identify likely FRBs, which means that the trained models should avoid missing any FRBs or mislabeling RFI as an FRB as much as possible. We used accuracy, recall and precision based on the confusion matrix to evaluate our models. Here, accuracy is the ratio of the number of correct predictions (of FRBs and non-FRBs) to the total number of predictions, which represents the ability to correctly classify samples. Recall is a measure of the sensitivity of a model for FRBs, which is given by the ratio of the number of correct FRB predictions to the total number of FRBs. Precision is the number of correctly predicted FRBs divided by the total number of predicted FRBs, which is the detection percentage for searching FRBs in observational data. A perfect precision of 1 means that every detection is actually an FRB, and no RFI is mistakenly predicted as FRB.

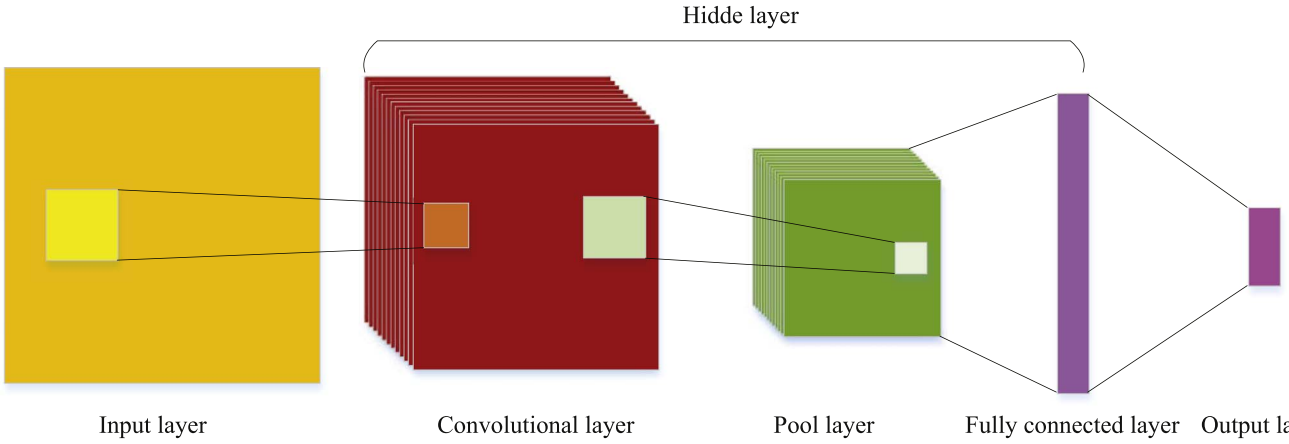


**Figure 5.** A schematic diagram for a convolutional neural network.

### *4.3. Training and Testing*

We prepared the data set with more than 150,000 samples, of which half were simulated FRB events. The data set was then split into training and testing sets, which encompassed 90% and 10% of the data, respectively. The cross-validation was conducted to assess the ability of the classifier during the training process, and 10% of the training set was allocated as a validation set. We trained our models on an Nvidia GTX 1080 GPU. After about six epochs, the accuracy, precision and recall of ResNetv2 and Xception classifiers could achieve above 99.7% with a confidence of 0.5. The test results for the classifier and the training time are displayed in Table 1.

Searching raw data with a classifier based on a neutral network is much faster than the dedispersion algorithm with different DM tries. The detection speed of our classifier is more than 15 times faster than the observation with one Nvidia GTX 1080 GPU. However, the DDSS pipeline needs additional time to do RFI mitigation and data processing. This can be resolved and optimized in real-time processing by parallelizing the data preprocessing. Overall, the DDSS pipeline provides an absolute advantage in speed for the implementation of voltage data dump.

## 5. Evaluation with Single Pulses from a Pulsar and Real FRB Events

All the FRB samples in the training set are generated through simulation. To verify the validity of our deep learning classifier in real observation data, we applied the classifier to detect the single pulses from PSR J1935+1616. The pipeline outputted 266 candidates, only one of which was a false positive. The precision of the classifier for this test is above 99.6%. Our analysis also found that the classifier can detect the pulses with the full-band frequency integrated S/N below 5. The classifier has good sensitivity to detect single pulses with low S/N. Here, we cannot take this S/N as the metric for model detection

**Table 1**
The Corresponding Metrics for ResNet18v2 and Xception Models on Test Set

| Network Model | Accuracy | Recall | Precision | Training Duration |
|---|---|---|---|---|
| ResNet18v2 | 99.89% | 99.78% | 100% | 330 minutes |
| Xception | 99.95% | 99.94% | 99.95% | 222 minutes |

sensitivity of signal intensity. This is because the weak pulses, with full-band frequency, may have the same level of full-band frequency integrated S/N as the band-limited strong pulses. The deep learning model for FRB searching tends to identify the morphology of the bursts rather than the signal strengths. Therefore, in theory, a deep learning model can achieve better accuracy and lower false positive rate than an S/N threshold-based dedispersion search in theory (Zhang et al. 2018).

Since February 2022, the repeating source FRB 20201124A has entered a new period of high activity. FAST has detected more than three thousand bursts from FRB 20201124A. (Wang et al. 2022). At the end of February, we observed FRB 20201124A using NSRT with an optimized XFB backend. On March 13, we detected a radio burst emitting from FRB 20201124A with BEAR and the DDSS pipeline in the observations conducted on 2022 February 28, for the first time (Yuan et al. 2022). Then we conducted a targeted monitoring of the FRB 20201124A for a few hours a day from March 16 to 23, and during that time, we detected radio bursts from FRB 20201124A in the NSRT observations on March 17, March 19 and March 20. As shown in Figure 6, the width, S/N, flux and frequency distribution of these bursts show diversity. The DDSS pipeline can detect all the bursts from the observations. This indicates that the DDSS pipeline has good generalization ability. Some basic information on these bursts is shown in Table 2, and a more detailed analysis will be presented in a subsequent paper.

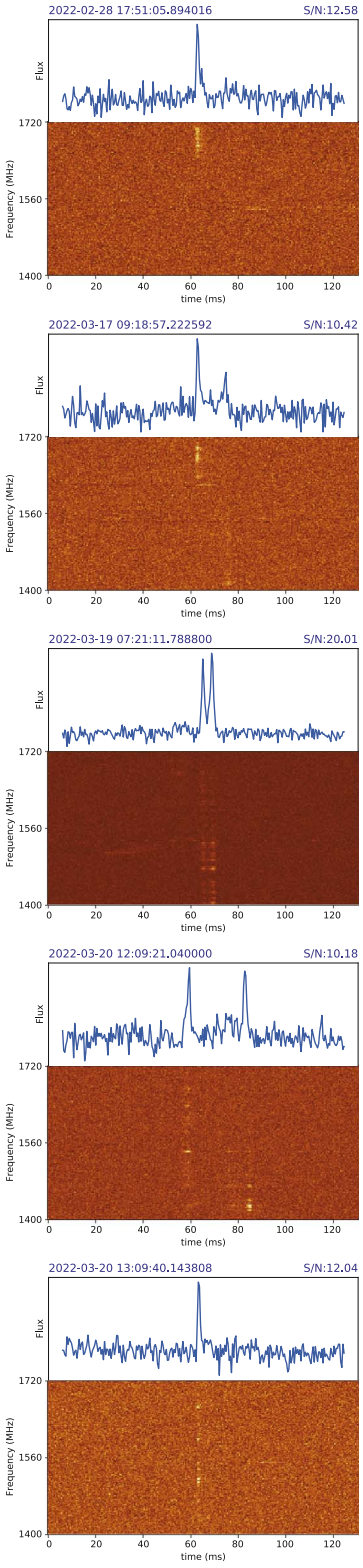


**Figure 6.** De-dispersed dynamic spectra of the bursts from FRB 20201124A with a DM of 411 pc cm$^{-3}$.

These FRBs were recorded in five filterbank files that contained a total of 22.5 minutes of observations. In this paper, we used these data files to conduct a comparative experiment with different deep learning models trained by simulated FRBs over different ranges of DM. The results are displayed in Table 3. In our experiment, the network models for FRB 20201124A trained with simulated FRBs in the range of 410–415 pc cm$^{-3}$ produced the best precision, which greatly reduced manual review. This kind of model is ideal for searching repeating FRBs. In addition, we found that the false positives came mainly from the observational data produced on 2022 March 17. Their dynamic spectra were populated with periodic wide-band strong impulsive RFI, even though the RFI mitigation techniques described in Section 3.2 were applied (see Figure 7). This kind of FRI is difficult to remove completely from the data through the current adoptive methods. Due to the intermittency of this RFI, it is also rarely present in the training set. This means that it would be difficult for the deep learning model to gain the ability to reject such cases. However, it is not a big problem for our purposes. The false alarms generated by this type of RFI are still within an acceptable range. For example, the DDSS pipeline returned only six false positives while conducting a search from about 7 hr of observations on 2022 March 21.

## 6. Conclusions and Future Work

We have described the DDSS pipeline based on deep learning, and presented the search results of the FRBs from FRB 20201124A in the observational data obtained from the NSRT at XAO. The results indicate that our DDSS pipeline can accurately search for FRB events with minimal manual review. A deep learning classifier for FRB search is faster and more accurate than the traditional method, especially for raw data. Moderate RFI mitigation is very important for greatly improving the performance of the deep learning classifier.

At present, the DDSS pipeline is just an offline search pipeline. We continue to develop more functions to improve the performance of this pipeline. We plan to design a ring buffer on the data processing server to facilitate the raw data transmission from XFB backend via optic fiber using 10 Gigabit Ethernet. The pipeline directly reads the raw spectrogram data from the ring buffer and classifies them in real-time. On the other hand, we will also continue to improve the accuracy and recall of the deep learning classifier by further optimizing the training set. The false positives we have detected will be put back into the training set as negative samples to retrain our model. A larger training set including simulated FRBs with a wider range of DMs will be built and

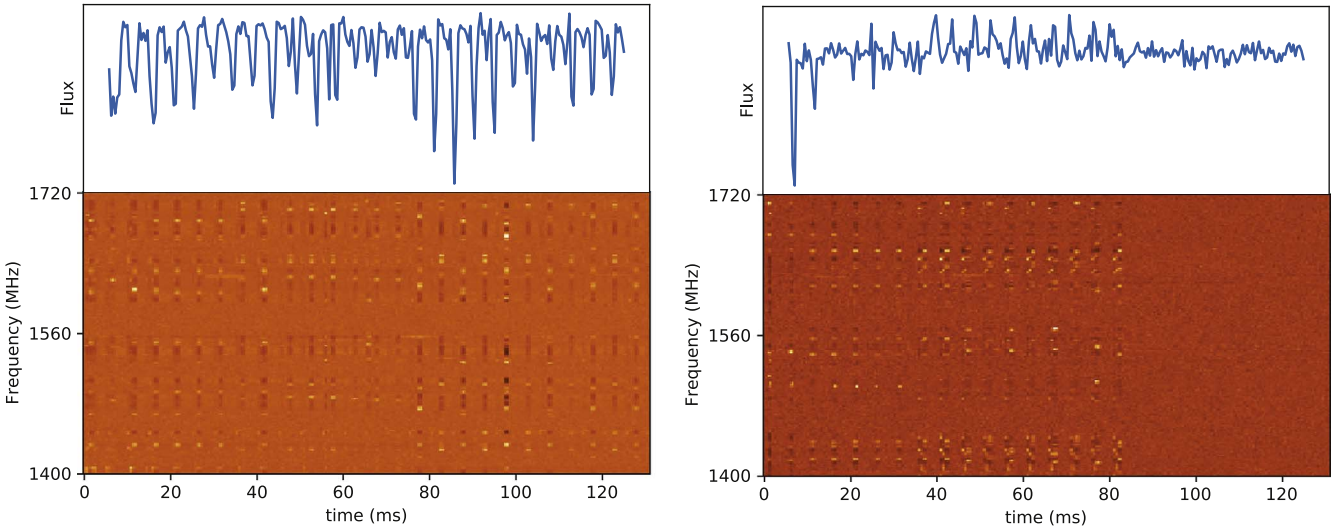


**Figure 7.** Two examples of the false positives after RFI mitigation.

**Table 2**
FRBs Emanating from FRB 20201124A Reported in this Paper

| Data | Time (UTC) | S/N[a] | Notes |
|---|---|---|---|
| 2022-2-28 | 17:51:05 | 12.58 | The first FRB detected by NSRT. |
| 2022-3-17 | 09:18:57[b] | 10.42[c] | Include two bursts, of which the low-frequency one was also detected by FAST during simultaneous observations (Wang et al. 2022). |
| 2022-3-19 | 07:20:01 | 20.01 | Burst with double-peak structure. |
| 2022-2-20 | 12:09:21[b] | 10.18[c] | Include two bursts, the time interval of which is more than 25 ms. |
| 2022-2-20 | 13:09:40 | 12.04 | A relatively narrow-band burst compared with others detected by the NSRT. |

**Notes.**
[a] The full-band frequency integrated S/N.
[b] The UTC of the left burst.
[c] The S/N value of the left burst.

**Table 3**
The Results of the Comparative Experiment

| Model | DM Range of Simulated FRBs | Candidates | FRBs | RFI | Precision |
|---|---|---|---|---|---|
| Xecption | 100–500 | 20 | 5 | 15 | 20.0% |
| Xecption | 410–415 | 5 | 5 | 5 | 100% |
| ResNet18v2 | 100–500 | 11 | 3 | 8 | 27.0% |
| ResNet18v2 | 410–415 | 8 | 7 | 1 | 87.5% |

used to train the model to acquire a classifier for more FRBs, which is suitable for blind FRB searching. With the completion of the real-time processing program development, we plan to conduct a commensal search for transient dispersed pulses with the NSRT in the near future.

## Acknowledgments

The authors are grateful to the members of the FAST FRB key science project for useful discussions about the bursts of FRB 20201124A detected by the NSRT. Y.L. would like to thank Heng Xu for further discussions about the bursts reported in this paper. Y.L. also thanks Yunpeng Men for providing the support of RFI mitigation with the ZDMF algorithm. We appreciate the referee for valuable comments which improved the presentation of the paper. This work is supported by the National Natural Science Foundation of China (Grant No. 11903071) and the Operation, Maintenance and Upgrading Fund for Astronomical Telescopes and Facility Instruments, budgeted from the Ministry of Finance (MOF) of China and administered by the Chinese Academy of Sciences (CAS).

## References


Abadi, M., Agarwal, A., Barham, P., et al. 2016, arXiv:1603.04467

Agarwal, D., Aggarwal, K., Burke-Spolaor, S., Lorimer, D. R., & Garver-Daniels, N. 2020a, MNRAS, 497, 1661

Agarwal, D., Lorimer, D. R., Surnis, M. P., et al. 2020b, MNRAS, 497, 352

Amiri, M., Andersen, B. C., Bandura, K., et al. 2021, ApJS, 257, 59

Amiri, M., Bandura, K., Berger, P., et al. 2018, ApJ, 863, 48

Amiri, M., Bandura, K., Bhardwaj, M., et al. 2019, Nature, 566, 230

Bannister, K. W., Shannon, R. M., Macquart, J. P., et al. 2017, ApJL, 841, L12

Barsdell, B. R., Bailes, M., Barnes, D. G., & Fluke, C. J. 2012, MNRAS, 422, 379

Bassa, C. G., Pleunis, Z., & Hessels, J. W. T. 2017, A&C, 18, 40

Caleb, M., Flynn, C., Bailes, M., et al. 2016, MNRAS, 458, 718

Chatterjee, S. 2021, A&G, 62, 29

Chollet, F. 2017, in 2017 IEEE Conf. on Computer Vision and Pattern Recognition (CVPR) (Piscataway, NJ: IEEE), 1800

Chollet, F., et al. 2015, Keras, https://keras.io

Connor, L., & van Leeuwen, J. 2018, AJ, 156, 256

Cordes, J. M., & Chatterjee, S. 2019, ARA&A, 57, 417

Eatough, R. P., Keane, E. F., & Lyne, A. G. 2009, MNRAS, 395, 410

Farah, W., Flynn, C., Bailes, M., et al. 2019, MNRAS, 488, 2989

Foster, G., Karastergiou, A., Golpayegani, G., et al. 2018, MNRAS, 474, 3847

He, K. M., Zhang, X. Y., Ren, S. Q., & Sun, J. 2016a, in 2016 IEEE Conf. Computer Vision and Pattern Recognition (CVPR) (Piscataway, NJ: IEEE), 770

He, K. M., Zhang, X. Y., Ren, S. Q., & Sun, J. 2016b, Computer Vision – ECCV 2016, 9908, 630

Huang, G., Liu, Z., Van Der Maaten, L., & Weinberger, K. Q. 2017, in 2017 IEEE Conf. Computer Vision and Pattern Recognition (CVPR) (Piscataway, NJ: IEEE), 2261

Li, C. K., Lin, L., Xiong, S. L., et al. 2021, NatAs, 5, 378

Lorimer, D. R., Bailes, M., McLaughlin, M. A., Narkevic, D. J., & Crawford, F. 2007, Science, 318, 777

Marcote, B., Nimmo, K., Hessels, J. W. T., et al. 2020, Nature, 577, 190

Masui, K., Lin, H. H., Sievers, J., et al. 2015, Nature, 528, 523

Men, Y. P., Luo, R., Chen, M. Z., et al. 2019, MNRAS, 488, 3957

Michilli, D., Hessels, J. W. T., Lyon, R. J., et al. 2018, MNRAS, 480, 3457

Morello, V., Rajwade, K. M., & Stappers, B. W. 2022, MNRAS, 510, 1393

Niu, C. H., Li, D., Luo, R., et al. 2021, ApJL, 909, L8

Petroff, E., Hessels, J. W. T., & Lorimer, D. R. 2019, A&ARv, 27, 4

Pilia, M., Burgay, M., Possenti, A., et al. 2020, ApJL, 896, L40

Ransom, S. 2001, New search techniques for binary pulsars, Thesis, Harvard University

Shannon, R. M., Macquart, J. P., Bannister, K. W., et al. 2018, Nature, 562, 386

Simonyan, K., & Zisserman, A. 2014, arXiv:1409.1556

Spitler, L. G., Cordes, J. M., Hessels, J. W. T., et al. 2014, ApJ, 790, 101

Thornton, D., Stappers, B., Bailes, M., et al. 2013, Sci, 341, 53

Wagstaff, K. L., Tang, B. Y., Thompson, D. R., et al. 2016, PASP, 128, 084503

Wang, P., Zhu, W. W., Zhang, Y. K., et al. 2022, ATel, 15288, 1

Xu, H., Niu, J. R., Chen, P., et al. 2022, Natur, 609, 685

Yuan, J. P., Li, J., Liu, Y. L., et al. 2022, ATel, 15289, 1

Zhang, B. 2020, Nature, 587, 45

Zhang, Y. G., Gajjar, V., Foster, G., et al. 2018, AJ, 866, 149

Zhu, W. W., Li, D., Luo, R., et al. 2020, ApJL, 895, L6